American Mineralogist, Volume 74, pages 956–959, 1989

LETTER

The ^{29}Si NMR shielding tensor in low quartz

Dane R. Spearing, Jonathan F. Stebbins
Department of Geology, School of Earth Sciences, Stanford University, Stanford, California 94305, U.S.A.

Abstract

The spatial orientation of ^{29}Si chemical shielding tensor in low quartz relative to the crystallographic axes has been determined by a least-squares fit and matrix diagonalization of the chemical shift vs. angle data for a single crystal of amethyst. The values for the principal shielding axes of the tensor are $\sigma_{11} = -102.6$, $\sigma_{22} = -107.0$, $\sigma_{33} = -109.1$ ppm. To within 6°, σ_{22} coincides with the **a** axis, and σ_{11} with the line defined by the intersection of the plane of the two longer Si–O bonds with the plane perpendicular to the **a** axis passing through the Si site. A similar relation holds for σ_{33} and the shorter Si–O distances. The data and orientations of the shielding tensor are consistent with previous studies that show the magnitude of the chemical shift to be inversely proportional to the Si–O bond distance. ^{29}Si NMR spectra taken from two orientations of a foliated quartzite show that the difference in the chemical shifts is consistent with the optical determination of the orientation of the quartz crystallites in the sample.

Introduction

NMR spectroscopy has become an increasingly important technique in determining the structural details of crystalline and amorphous silicates (Kirkpatrick, 1988; Stebbins, 1988). Most recent studies have used the magic-angle-spinning (MAS) technique to observe relatively narrow lines and the isotropic average of the chemical shift. However, a complete description of the chemical shift for a given site contains much additional information on the symmetry and orientation of the local electron distribution, and is conveniently represented by a second-rank tensor. The chemical shift δ for a nucleus with a noninteger spin in a given site is defined by $\delta = k\mathbf{I}\cdot\hat{\sigma}\cdot\mathbf{H}_0$, where k = constant for a given nucleus, $\mathbf{I}$ = nuclear spin vector, $\hat{\sigma}$ = chemical shift anisotropy (CSA) tensor, and $\mathbf{H}_0$ = magnetic field vector. Experimentally, δ is measured relative to the NMR transition in some reference compound and is expressed as a normalized difference $\delta = (\nu - \nu_{ref})/\nu_{ref}$, where ν and ν_{ref} are the frequencies at which the NMR transition of the spin of interest occurs in the sample and the standard, respectively. Units for δ are typically given in parts per million (ppm). In order to understand the mechanisms that can affect the chemical shift, one must know how the nuclear-spin and magnetic-field vectors interact because these two vectors are related by the CSA tensor. This tensor can be diagonalized to yield three mutually perpendicular eigenvectors called the principle shielding axes with the conventions that $|\sigma_{33}| > |\sigma_{22}| > |\sigma_{11}|$ and that the sign of σ is the same as that of the chemical shift δ. The principal values of the tensor can often be approximated from the position of spinning sidebands in a MAS experiment (Smith et al., 1983) or from static powder spectra (Grimmer et al., 1981). In the general case of low local symmetry, the only way in which the CSA tensor (or chemical shielding ellipsoid) can be completely defined spatially relative to the structural axes within a crystal is through single-crystal static NMR. The isotropic chemical shift can in turn be related to the CSA tensor by $\delta_{iso} = (\sigma_{11} + \sigma_{22} + \sigma_{33})/3$.

Previous experiments have shown that the shortest Si–O bond distances correspond with the largest ^{29}Si chemical shift (Grimmer, 1985; Grimmer et al., 1981; Smith et al., 1983); however, only one other study has used single-crystal NMR spectroscopy to directly measure the chemical shift relative to crystallographic orientation in a silicate (Weiden and Rager, 1985). The techniques applied to this study have been used extensively for a number of organic compounds (Kempf et al., 1972; Pausak et al., 1973), inorganic solids (Gibby et al., 1972), and several nonsilicate minerals (Lauterbur, 1958; McKnett et al., 1975). Quartz was chosen because of its simple composition (one unique SiO_4 tetrahedron per unit cell) and the nonuniaxial point symmetry of the Si–O tetrahedra (i.e., the symmetry axis through the Si site does not coincide with any of the Si–O bonds). So far, no other single-crystal static NMR study has been done on a tectosilicate, and the goal of this experiment is to understand the relationship between chemical shift and structure in other silicates. This may be particularly important in under-

0003–004X/89/0708–0956$02.00

standing static powder spectra, which have been shown in some cases to be very useful in characterizing silicate glass structure (Brandriss and Stebbins, 1988).

Experimental procedure

For the single-crystal study of the ^{29}Si chemical shift tensor in low quartz, three mutually perpendicular cores were drilled from a single crystal of clear amethyst: one each parallel to the **a**, **c**, and **a*** (perpendicular to **a**) axes. Each core was approximately 10 mm long and 4 mm in diameter. (Amethyst was used instead of pure colorless quartz in the expectation that the Fe impurities would shorten the spin-lattice relaxation time, which unfortunately remained on the order of several hours.) The experiments were conducted at room temperature on a Varian VXR-400 spectrometer with a ^{29}Si Larmor frequency of 79.459 MHz, using a 5-mm-diameter horizontal solenoid probe. The sample was allowed to relax for 3 to 12 h in the magnet before receiving a single 90° pulse (3 μs). Each sample was rotated about its long axis perpendicular to the external magnetic field $\mathbf{H}_0$, and spectra were taken at 15° intervals over a 180° range (with the exception of the sample with a cylindrical axis parallel to **c**, which was observed over a 90° range). The accuracy of the rotation angle θ was $\pm 5°$. Line widths were about 1 ppm, and the chemical shift δ of each was measured to ± 0.2 ppm relative to tetramethylsilane (TMS). Results for the three rotations are shown in Figure 1, where the points denote the experimental values and the solid curves represent a least-squares fit of the data using the function

$$\delta(\theta) = \delta_1 \sin^2\theta + 2\delta_2 \sin\theta \cos\theta + \delta_3 \cos^2\theta.$$

MAS spectra of the amethyst sample were taken using a Varian MAS probe at a spinning speed of 4.5 MHz.

As an application of this technique, spectra taken at specific orientations from a foliated quartzite sample were compared with an optical determination of the crystallite alignment. The sample is a ductilely deformed mylonite from the northern Snake Range metamorphic core complex, Nevada, and is described in detail by Lee et al. (1987). A strong c-axis fabric was observed optically, with a high preference of the axes to form a plane at right angles to both the foliation and lineation. A core was drilled from the quartzite parallel to the foliation direction, and spectra were taken in two orientations: one with the foliation plane parallel to $\mathbf{H}_0$, the other perpendicular.

Analysis of single-crystal data

When observed with the **c** axis perpendicular to the external magnetic field ($\mathbf{H}_0 \perp \mathbf{c}$), all Si atoms within the quartz unit cell are magnetically equivalent, resulting in a single ^{29}Si NMR signal (Fig. 1C). In this orientation, the chemical shift is constant and independent of rotation about **c**. This implies that one of the circular cross sections of the chemical shift tensor is in the **a**-**a*** plane, and that one of the eigenvectors of the tensor must also lie in this plane. For the orientation $\mathbf{H}_0 \perp \mathbf{a}$, two peaks are observed, indicating two magnetically inequivalent Si atoms per unit cell. One of those two peaks combines the signal from two magnetically equivalent Si sites and was determined from its greater intensity and by the slight splitting of the peak at high angles of **a** with $\mathbf{H}_0$. (The splitting of one of the peaks in Fig. 1A above 150° is interpreted as being due to the slight distortion from a perfect hexagonal arrangement of the Si atoms that is exhibited in the low quartz structure. Hence, when **a** is parallel to $\mathbf{H}_0$, the two Si atoms not lying along that particular **a** axis are not magnetically equivalent, and their respective chemical shifts should show a slight deviation from one another. However, this deviation is on the order of the error associated with the curve fitting and angular precision in this experiment, and these two Si atoms have been treated as magnetically equivalent sites for the purpose of calculating the average chemical shift ellipsoid. No explanation is given here for the splitting of the central symmetric curve below 45° in Figure 1B. A high-temperature single-crystal NMR experiment on high quartz could be useful here.) For $\mathbf{H}_0 \perp \mathbf{a}^*$, three peaks are observed. Note that for both the rotation about the **a** axis and about **a***, the curves cross over at the 0°, 90°, and 180° positions (i.e., they are magnetically equivalent at these positions), which is consistent with the observation that the chemical shift is constant when $\mathbf{H}_0$ is perpendicular to **c**.

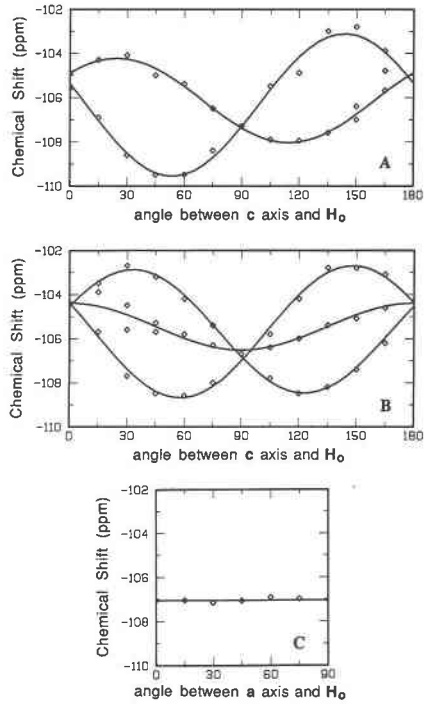

Fig. 1. Plot of chemical shift vs. angle (in degrees) for rotation about the **a** (A), **a*** (B), and **c** (C) axes.

These data are consistent with the crystal structure of low quartz. There is only one crystallographically unique Si site in the quartz structure that is related to all other Si atoms in the unit cell through a 3-fold screw axis parallel to **c**. The three Si atoms in the unit cell are not, however,

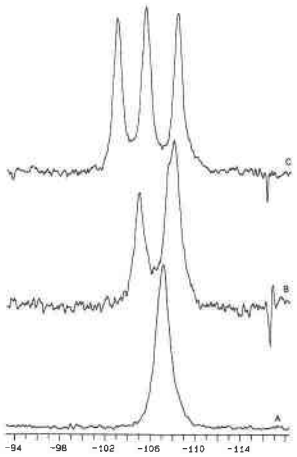

Fig. 2. Single-crystal static ^{29}Si spectra of low quartz. (A) **c** $\perp$ $\mathbf{H}_0$, and **a** $\wedge$ $\mathbf{H}_0 = 0°$. (B) **a** $\perp \mathbf{H}_0$ and **c** $\wedge$ $\mathbf{H}_0 = 135°$. (C) **a*** $\perp \mathbf{H}_0$ and **c** $\wedge$ $\mathbf{H}_0 = 135°$. Note that when **c** $\perp \mathbf{H}_0$, all Si sites are magnetically equivalent, and only one peak is present. When **a** $\perp$ $\mathbf{H}_0$, two of the Si sites are magnetically equivalent resulting in two peaks, one more intense than the other. For **a*** $\perp \mathbf{H}_0$, and any general orientation, there are three magnetically inequivalent Si sites resulting in three distinct NMR peaks (chemical shifts in ppm relative to tetramethysilane).

magnetically equivalent for orientations with respect to an arbitrary external magnetic-field axis. The ellipsoid defined by the CSA tensor is identical in shape for each Si in the crystal, but lies in one of three different absolute orientations. Thus, in a general orientation, three NMR peaks are present. This number is reduced to two or one in special orientations. Examples of ^{29}Si NMR spectra from three orientations of low quartz are given in Figure 2.

Through matrix diagonalization, a set of eigenvectors and eigenvalues was determined for each CSA tensor associated with each one of the three Si atoms within the unit cell. These were then referenced to the **a** axis passing through each Si site, and the average was calculated (Table 1). Associated errors for the eigenvectors, eigenvalues, and angles relative to the reference axis **a** were determined from the least-squares fit of the data and by propagating the $\pm 5°$ error in orientation through the eigenvalue calculations.

The isotropic chemical shift (δ_{iso}) was calculated to be -106.3 ± 0.5 ppm by using the mean principal shielding axes as determined above. Previous experimental determinations for δ_{iso} have yielded values of -107.1 ppm to -107.4 ppm (Lippmaa et al., 1980; Smith and Blackwell, 1983; Ramdas and Klinowski, 1984), which differs from our calculated value. However, experimental MAS spectra of the amethyst used for this experiment yield a δ_{iso} value of -107.0 ± 0.2 ppm. This difference between the experimentally and theoretically determined δ_{iso} is most likely due to the $\pm 5°$ error in orientation propagated through the matrix diagonalization calculations, giving rise to the uncertainty in the position of the principal shielding axes.

TABLE 1. Mean eigenvectors of the ^{29}Si shielding ellipsoid in low quartz relative to associated **a** axis

	σ_{11} = −102.6(1)	σ_{22} = −107.0(4)	σ_{33} = −109.1(2)
x	0.008(48)	0.997(3)	0.029(65)
y	0.559(10)	0.027(33)	0.828(7)
z	0.828(7)	0.010(74)	−0.557(8)
θ	89(5)	1.6(4.0)	88(5)
ϕ	56(4)	0.6(3.0)	−34(4)

Note: θ = angle between eigenvector and **a** axis in **a**-**a*** axial plane. ϕ = angle between eigenvector and **a**-**a*** axial plane. σ in ppm; ϕ and θ in degrees.

Discussion

^{29}Si is a dilute (4.7% natural abundance), spin ½ isotope. In a system where other nuclear spins (e.g., ^{17}O) and unpaired electron spins (e.g., Fe^{3+}) are of low abundance, such as in SiO_2, the NMR spectrum is mainly controlled by the chemical shift interaction. This, in turn, is dominated by the local geometry of the crystal structure.

Given that there is no single unique Si–O bond within the tetrahedra in the quartz structure (i.e., the tetrahedra do not exhibit uniaxial symmetry), one would not expect any of the eigenvectors of the CSA tensor to lie along any of the Si–O bonds, and this is indeed the case. Instead, we find that the direction of σ_{11} is nearly coincidental with the line defined by the intersection of the plane of the two longer Si–O bonds with the plane perpendicular to the **a** axis passing through the Si site. A similar relation holds for σ_{33} and the shorter Si–O distances (Fig. 3). The intermediate eigenvector σ_{22}, within experimental error, coincides with the **a** axis passing through the Si atom. Hence, the magnitude of the chemical shift δ observed relative to the two different Si–O bond lengths in quartz is consistent with that of previous studies (Grimmer et al., 1981; Dupree and Pettifer, 1984; Ramdas and Klinowski, 1984; Grimmer, 1985) in that δ increases with decreasing bond length. The nearly spherical shape of the CSA tensor is also in agreement with that predicted by Grimmer (1985) for framework silicates (Q^4 speciation of the Si atoms). The eigenvectors do not exactly coincide with the lines mentioned above since the eigenvectors are mutually perpendicular, whereas the angle between the projections of the Si–O bonds is slightly greater than 90°, reflecting the slight distortion of the tetrahedra in the quartz structure. However, within experimental error, the eigenvectors are nearly coincidental with the short and long Si–O bond-length projections.

The point symmetry of the CSA tensor should also be consistent with that of the Si site. This is indeed the case: one of the circular sections of the tensor ellipsoid lies within the **a**-**a*** plane, and one of the principal values of the chemical shielding tensor (σ_{22}) is coincident with the 2-fold axis, which is consistent with the Si point symmetry of 2.

Application

^{29}Si NMR spectra were taken in two orientations from the foliated quartzite sample described previously: one

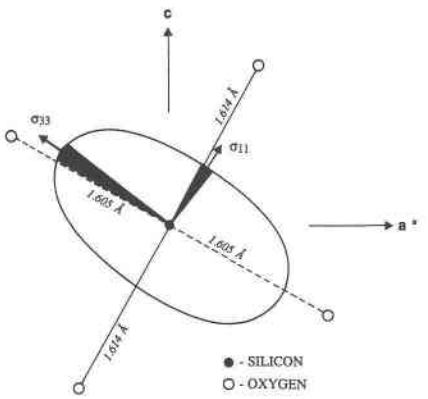

Fig. 3. A cross section of chemical shielding ellipsoid through a plane perpendicular to the **a** axis associated with the Si site. Relative magnitudes of principal shielding axes (σ_{11} and σ_{33}) have been greatly exaggerated to show their relationship to Si–O bonds, which have been projected onto this plane for comparison. Dashed bond lines indicate the bond is going into the plane, and solid lines indicate the bond is coming out of the plane. Solid angles represent experimental error associated with principal shielding axes. Bond lengths for low quartz from Louise et al. (1980).

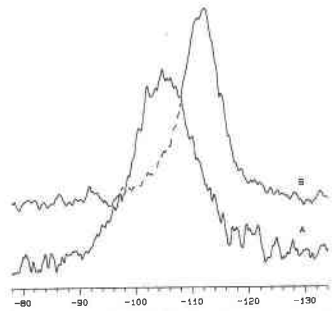

Fig. 4. Static spectra of highly deformed quartzite. (A) quartz **c** axes are preferentially oriented in a plane parallel to $\mathbf{H}_0$ and thus are at all angles to $\mathbf{H}_0$. (B) **c** axes lie in a plane at right angles to $\mathbf{H}_0$, restricting their angular distribution and changing their average chemical shift (in ppm).

with the foliation plane parallel to $\mathbf{H}_0$, the other perpendicular. Figure 4 clearly shows that this orientational difference can be observed through static ^{29}Si NMR spectroscopy. In the orientation where the foliation plane is parallel to $\mathbf{H}_0$, a greater chemical shift is observed, indicating that the plane defined by the **c** axes is perpendicular to the magnetic-field vector, whereas a lesser shift is observed when the foliation plane is perpendicular to $\mathbf{H}_0$ suggesting that the "**c** plane" is parallel to $\mathbf{H}_0$. In the former case, the line is relatively narrow as would be expected if most of the axes are at right angles to $\mathbf{H}_0$; in the latter case, the peak is broader since the **c** axes can be at any angle to $\mathbf{H}_0$. These data agree with the orientation as determined optically. As suggested by this experiment, one possible application of single-crystal static NMR spectroscopy is the determination of the orientation of a single or large number of crystals where optical determination is not possible owing to the size or opaqueness of the sample.

Acknowledgments

This work was supported by NSF grants EAR-87-07175 and EAR-85-53024. We would like to thank Jeff Lee for the use of his quartzite samples, Gordon Brown and Ian Farnan for their assistance and comments, and Subrata Ghose for a constructive review of the manuscript.

References cited

Brandriss, M.E., and Stebbins, J.F. (1988) Effects of temperature on the structure of silicate liquids: ^{29}Si NMR results. Geochimica et Cosmochimica Acta, 52, 2659–2669.

Dupree, E., and Pettifer, R.F. (1984) Determination of the Si–O–Si bond angle distribution in vitreous silica by magic angle spinning NMR. Nature, 308, 523–525.

Gibby, M.G., Pines, A., Rhim, W.-K., and Waugh, J.S. (1972) ^{31}P chemical shielding anisotropy in solids. Single crystal and powder studies at 99.4 MHz. Journal of Chemical Physics, 56, 991–995.

Grimmer, A.-R. (1985) Correlation between individual Si–O bond lengths and the principal values of the ^{29}Si chemical shift tensor in solid silicates. Chemical Physics Letters, 119, 416–420.

Grimmer, A.-R., Peter, R., Fechner, E., and Molgedey, G. (1981) High-resolution ^{29}Si NMR in solid silicates. Correlations between shielding tensor and Si–O bond length. Chemical Physics Letters, 77, 331–335.

Kempf, J., Speiss, H.W., Haeberlen, U., and Zimmermann, H. (1972) ^{13}C anisotropic chemical shift in a single crystal of benzophenone. Chemical Physics Letters, 17, 39–42.

Kirkpatrick, R.J. (1988) MAS NMR spectroscopy of minerals and glasses. In F.C. Hawthorne, Ed., Spectroscopic methods in mineralogy and petrology. Mineralogical Society of America Reviews in Mineralogy, 18, 405–427.

Lauterbur, P.C. (1958) Anisotropy of the C^{13} chemical shift in calcite. Physical Review Letters, 1, 343–344.

Lee, J., Miller, E.F., and Sutter, J.F. (1987) Ductile strain and metamorphism in an extentional tectonic setting: A case study from the northern Snake Range, Nevada, USA. In M.P. Coward, J.F. Dewey, and P.L. Hancock, Eds., Continental extention tectonics. Geological Society Special Publication no. 28, 267–298. Blackwell, Oxford.

Lippmaa, E., Mägi, M., Samoson, A., Engelhardt, G., and Grimmer, A.-R. (1980) Structural studies of silicates by solid-state high-resolution ^{29}Si NMR. Journal of the American Chemical Society, 102, 4889–4893.

Louise, L., Prewitt, C.T., and Weidner, D.J. (1980) Structure and elastic properties of quartz at pressure. American Mineralogist, 65, 920–930.

McKnett, C.L., Dybowski, C.R., and Vaughan, R.W. (1975) High resolution proton NMR study of gypsum, $CaSO_4 \cdot 2H_2O$. Journal of Chemical Physics, 63, 4578–4581.

Pausak, S., Pines, A., and Waugh, J.S. (1973) Carbon-13 chemical shielding tensors in single-crystal durene. Journal of Chemical Physics, 59, 591–595.

Ramdas, S., and Klinowski, J. (1984) A simple correlation between isotropic ^{29}Si-NMR chemical shifts and T–O–T angles in zeolite frameworks. Nature, 308, 521–523.

Smith, J.V., and Blackwell, C.S. (1983) Nuclear magnetic resonance of silica polymorphs. Nature, 303, 223–225.

Smith, K.A., Kirkpatrick, R.J., Oldfield, E., and Henderson, D.M. (1983) High-resolution silicon-29 nuclear magnetic resonance spectroscopy study of rock-forming silicates. American Mineralogist, 68, 1206–1215.

Stebbins, J.F. (1988) NMR spectroscopy and dynamic processes in mineralogy and geochemistry. In F.C. Hawthorne, Ed., Spectroscopic methods in mineralogy and petrology. Mineralogical Society of America Reviews in Mineralogy, 18, 405–427.

Weiden, N., and Rager, H. (1985) The chemical shift of the ^{29}Si nuclear magnetic resonance in a synthetic single crystal of Mg_2SiO_4. Zeitschrift für Naturforschung, 40a, 126–130.

Manuscript received April 26, 1989
Manuscript accepted May 5, 1989